ISSN 1990-7478, Biochemistry (Moscow), Supplement Series A: Membrane and Cell Biology, 2022, Vol. 16, No. 1, pp. 91–105. © Pleiades Publishing, Ltd., 2022.
Russian Text © The Author(s), 2022, published in Biologicheskie Membrany, 2022, Vol. 39, No. 1, pp. 28–43.

Regulation of the Structural Stability of Erythrocytes by Hydrogen Peroxide: Mathematical Model and Experiment

V. V. Voinarouski[a], * and G. G. Martinovich[a]

[a] *Belarusian State University, Minsk, 220030 Belarus*

**e-mail: voynarovskiy@bsu.by*

Received March 28, 2021; revised July 26, 2021; accepted July 27, 2021

Abstract—In this study, the regulatory mechanisms induced by extracellular hydrogen peroxide were analyzed on the basis of a mathematical model that considers the key stages of the formation of methemoglobin and ferrylhemoglobin, as well as their binding to the erythrocyte membrane. Numerical modeling has shown that reversible binding of methemoglobin to the membrane is an adaptive mechanism aimed at stabilizing the lipid bilayer of the membrane. On the other hand, an increase in the concentration of ferrylhemoglobin and its binding to the membrane leads to an increase in pathophysiological processes that reduce the structural stability of cells. The quantity of methemoglobins and ferrylhemoglobins formed depends on the concentration of extracellular hydrogen peroxide and exposition time, the number of cells in the sample, the state of the antioxidant system of erythrocytes, the metabolic activity of cells and external metabolic conditions. Based on numerical modeling, optimal conditions (oxidant concentration and exposition time) have been determined, under which the activation of adaptive processes occurs. Experiments with erythrocyte hemolysis in vitro have shown that hydrogen peroxide at concentrations of 10–200 μM causes an increase in the structural stability of the membrane and a decrease in the proportion of hemolyzed erythrocytes.

Keywords: erythrocytes, hydrogen peroxide, methemoglobin, adaptation, hormesis

DOI: 10.1134/S1990747822010093

INTRODUCTION

The formation of reactive oxygen species (ROS) is an important phenomenon in cellular respiration, since it results in a wide range of physiological and pathophysiological consequences. Until recently, the exclusively pathological role of ROS was the dominant point of view; the formation of ROS was associated with the development of chronic and degenerative diseases. However, it is known nowadays that ROS are participants in numerous physiological processes, including regulation of metabolism, activation of adaptive mechanisms, triggering apoptosis, etc. [1–4].

According to modern concepts, hydrogen peroxide is the main molecule of the ROS group involved in regulatory processes [2]. Basic features of the signals transmitted by hydrogen peroxide are the threshold concentration of activation and exposure duration. The effect of such signals is reversible, as evidenced by the presence in the cell of a special set of enzymatic systems, including catalase (CAT), glutathione peroxidase (GPX), peroxyredoxin (PRX), etc. [2, 5–7]. A moderate increase in the concentration of hydrogen peroxide activates mechanisms associated with protection and adaptation [2–4]. These mechanisms control the balance of hydrogen peroxide formation and utilization, and violation of this balance leads to the development of various diseases [1, 3]. Thus, the effect of hydrogen peroxide on cells at low concentrations leads to adaptation and increased protection, while at high concentrations it causes damage to cellular structures. Such a property of living systems, described by a change in the sign of the biological effect with an increase in the activity/amount of the stressor, is termed hormesis and is explained by the presence of specific compensatory and adaptive mechanisms [8, 9].

Transcription factor Nrf2 (nuclear E2-related factor 2) plays the key role in the adaptation processes of most cells, the activity of which is regulated with the participation of the redox-dependent protein Keap1 (Kelch-like ECH-associating protein 1) [10, 11]. However, this system of maintaining redox homeostasis is absent in erythrocytes, and the nature of activation of adaptive processes of erythrocytes under oxidative stress remains unknown.

Erythrocytes are the most plentiful cells in the human body that perform a variety of functions related to homeostasis [9, 12, 13]. Changes in the functional state of the body, including those associated with a violation of redox homeostasis, would affect the state of erythrocytes; therefore, it is necessary to study the protective mechanisms of these cells and find ways to

regulate their functioning under oxidative stress. Normally, the concentration of hydrogen peroxide in the blood does not exceed 10 μM [14]. In pathophysiological processes, the extracellular concentration of hydrogen peroxide can increase up to 200–250 μM [15, 16]. The study of mechanisms of the adaptive response of erythrocytes to hydrogen peroxide in the concentration range from 10 to 250 μM was the purpose of this work.

Here we examined the role of hydrogen peroxide as a stimulating agent that increases the structural stability of human erythrocytes during oxidative hemolysis mediated by hypochlorous acid (HOCl). The cell destruction caused by HOCl is due to a colloidal osmotic mechanism with the formation of pores of high permeability [17]; therefore, an increase in the structural stability of the membrane may decrease the proportion of non-hemolyzed cells.

One of the most important mechanisms for increasing the structural stability of membranes is their interaction with the main protein of erythrocytes, hemoglobin [9]. Hemoglobin is a regulator of erythrocyte homeostasis and a key participant in intracellular oxidative processes [9, 12]. Binding of hemoglobin to the membrane regulates various intracellular processes, such as energy metabolism, membrane deformability, eryptosis, etc. Binding of hemoglobin with membrane proteins occurs due to covalent and non-covalent interactions and binding of hemoglobin with membrane lipids involves hydrophobic interactions [18–21]. The rate constants of formation and disruption of the hemoglobin–membrane complex depend on the state of hemoglobin [19, 21]. Binding constant of interaction of methemoglobin (MetHb), formed due to the oxidation of oxyhemoglobin, with the membrane components is the highest, suggesting a significant role of this reaction in regulating the stability of the membrane. The study of the molecular mechanisms of this interaction has shown that in the case of insignificant and reversible oxidation hemoglobin exerts a stabilizing effect on membranes, while the formation of ferrylhemoglobins (FerHB) under the oxidative stress impairs the interaction of the membrane with cytoskeleton [22]. Thus, the regulation of the oxidative metabolism of hemoglobin may underlie the hormesis effect produced by oxidants on erythrocytes.

Confirmation of this hypothesis can be carried out by constructing a mathematical model of intracellular processes based on known data. The beginning of the study of redox metabolism of erythrocytes using mathematical modeling can be attributed to the 60s of the last century. Nicholls described the processes of transport and utilization of hydrogen peroxide based on diffusion and decomposition of the oxidant by catalase [23]. In the early 2000s, modeling of hydrogen peroxide metabolism in erythrocytes was supplemented by complex processes associated with the oxidation of hemoglobin and its transition to oxidized forms [6]. At the same time, Kinoshita et al. proposed models for reduction processes, which considered the contribution of several ways of reducing oxidized forms of hemoglobin [24]. The energy for the reduction can be replenished only through glycolysis processes, the first models of which were developed in the 1980s in the groups of Rappoport–Yakobash [25] in Germany and of Ataullakhanov [26] in the USSR. In the following decades, mathematical models of glycolysis were upgraded and refined [24, 27]. In this study, the effect of pre-incubation of cells with hydrogen peroxide on the structural stability of erythrocytes during oxidative hemolysis was explored and a quantitative contribution of participants in hemoglobin metabolism to the regulation of the structural stability of membranes was assessed.

DESCRIPTION OF THE MODEL

A mathematical model was created describing the key stages of the formation of methemoglobin and ferrylhemoglobin and their binding to the membrane under the action of extracellular hydrogen peroxide. The model includes the processes of diffusion and utilization of hydrogen peroxide in the cell, the formation and reduction of methemoglobin and ferrylhemoglobin, the formation and disruption of the hemoglobin–membrane complex and the formation of reducing equivalents due to glycolysis. The general scheme of these processes is shown in Fig. 1. All equations and rates are presented in Table 1. Constants and initial conditions are given in Tables 2 and 3.

The rate of change in the concentration of extracellular hydrogen peroxide depends on its diffusion into cells and is described by Fick's first law for membranes [33]. The diffusion of the oxidant into the cell and its utilization causes a decrease in the extracellular concentration of H_2O_2 (v_1), which is directly proportional to the number of cells in the sample, and a change in the concentration of hydrogen peroxide in the intracellular medium (v_2).

In the cell, hydrogen peroxide is reduced to water with the participation of enzymes Cat and Gpx [7]. At high concentrations of hydrogen peroxide, Cat is the main participant in the H_2O_2 utilization, as the rate constant of this reaction is higher than that of other enzymes and at the same time it does not require additional substrates. Upon interaction with a molecule of hydrogen peroxide, a Cat molecule enters the Comp I (v_3) state; upon interaction with the next oxidizer molecule, it returns to its original state (v_4). Gpx (v_5) is an additional participant in the utilization; it catalyzes the reduction of hydrogen peroxide by intracellular glutathione (GSH), which is also used for the reduction of ascorbic acid (Asc) [31].

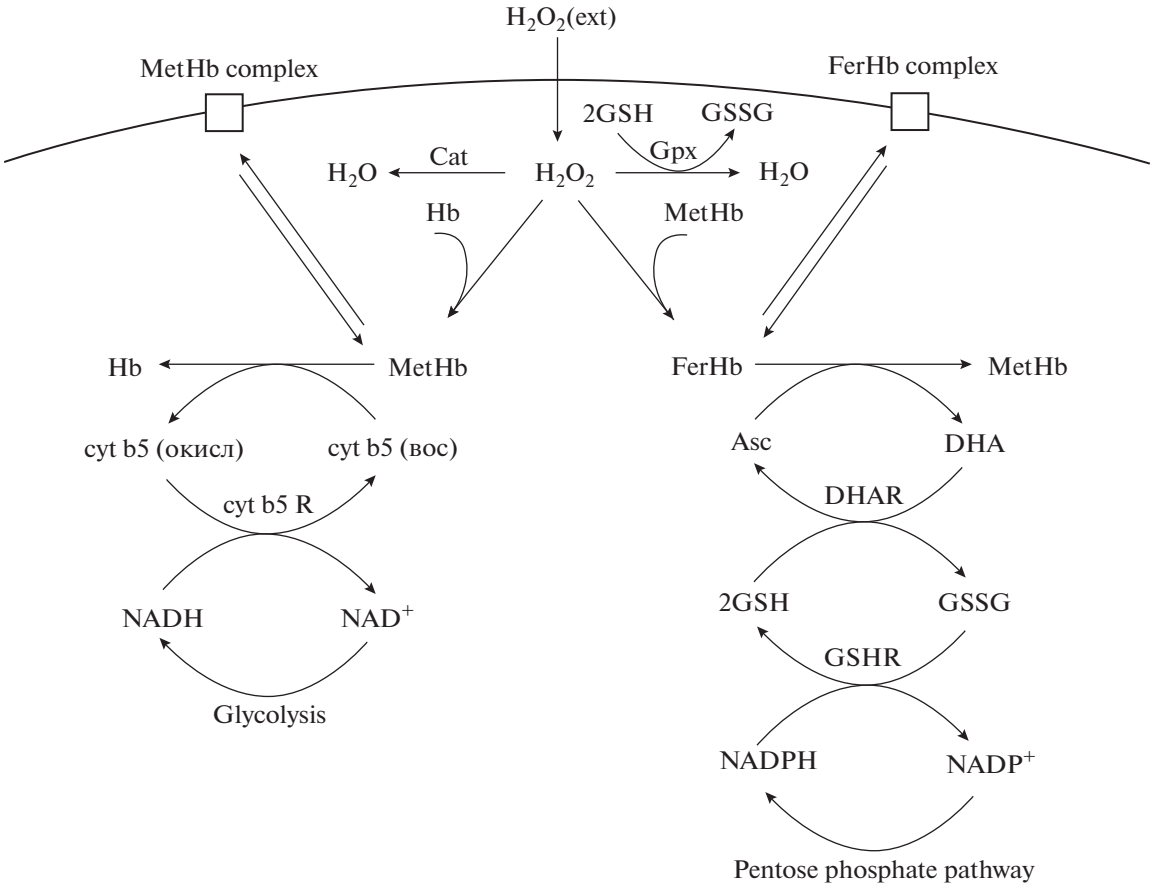

Fig. 1. The processes of erythrocyte metabolism with the participation of hydrogen peroxide considered in the model. Hb, hemoglobin; MetHb, methemoglobin; FerHb, ferrylhemoglobin; H_2O_2, hydrogen peroxide; H_2O_2 (ext), extracellular hydrogen peroxide; Cat, catalase; Gpx, glutathione peroxidase; GSH, glutathione; GSSG, glutathione disulfide; cyt b5 (ox), oxidized form of cytochrome b5; cyt b5 (red), reduced form of cytochrome b5; cyt b5 R, cytochrome b5 reductase; NAD^+/NADH, oxidized and reduced forms of nicotinamide adenine dinucleotide; Asc, ascorbic acid; DHA, dehydroascorbate; DHAR, dehydroascorbate reductase; GSHR, glutathione reductase; $NADP^+$/NADPH, oxidized and reduced forms of nicotinamide adenine dinucleotide phosphate; MetHb complex, membrane complex with methemoglobin; FerHb complex, membrane complex with ferrylhemoglobin.

The oxidation of hemoglobin with the formation of methemoglobin (v_6) [24, 34–36] and the oxidation of methemoglobin with the formation of ferrylhemoglobin (v_7) are competing processes involving hydrogen peroxide [6]. The rates of these processes, according to the law of acting masses, are proportional to the concentration of participants.

It was shown that at elevated concentrations of methemoglobin, the main way of its reduction is interaction with cytochrome b5 (v_8), which is then reduced by NADH with the participation of the cytochrome b5 reductase (cyt b5 R) (v_9) [24]. The reduction of ferrylhemoglobin is carried out by cellular antioxidants without the participation of enzymes. The model considers the reaction of ferrylhemoglobin with Asc, as its reaction constant has the highest value (v_{10}). When ascorbate is reduced, radicals are formed that rapidly dismutate to dehydroascorbate (DHA) in a direct reaction or with the participation of enzymes [37].

In this study, a complete model of glycolysis and the pentose phosphate pathway was constructed, the equations of which is presented in the Annex. The main contribution to the regulation of the NAD^+/NADH redox state is associated with reactions catalyzed by glyceraldehyde-3-phosphate dehydrogenase (GAPDH) and lactate dehydrogenase (LDH) [24, 32, 38]. The first reaction is one of the stages of glycolysis; it catalyzes the oxidation of glyceraldehyde-3-phosphate (gap) with the formation of 1,3-diphosphoglycerate (13pg) and the release of NADH. The second catalyzes the conversion of pyruvate (pyr) to lactate (lac) with the release of NAD^+. Under physiological conditions, this reaction proceeds in the direction of the formation of lactate and NAD^+ using the electrons released in the first reaction. Due to this, the ratio of concentrations [pyruvate] : [lactate] = 1 : 15 and of [NADH] : [NAD^+] = 1 : 600 is observed in erythrocytes [24, 32]. When the NADH concentration

Table 1. Reactions and velocity equations in the model

No.	Reaction	Velocity equation
1	$H_2O_2(ext) \rightarrow H_2O_2$	$v_1 = -P(H_2O_2 - H_2O_2(ext))\frac{S_{cell}}{V}N_{cell}$
2	$H_2O_2(ext) \rightarrow H_2O_2$	$v_2 = -P(H_2O_2 - H_2O_2(ext))\frac{S_{cell}}{V_{cell}}$
3	$H_2O_2 \xrightarrow{Cat} H_2O$	$v_3 = k_3 \cdot Cat \cdot H_2O_2$
4	$H_2O_2 \xrightarrow{ComplI} H_2O + O_2$	$v_4 = k_4 \cdot Compl \cdot H_2O_2$
5	$H_2O_2 + 2GSH \xrightarrow{Gpx} 2H_2O + GSSG$	$v_5 = \frac{Gpx \cdot GSH \cdot H_2O_2}{K_1 \cdot H_2O_2 + K_2 \cdot GSH}$
6	$2Hb + H_2O_2 \rightarrow 2MetHb + H_2O$	$v_6 = k_6 \cdot Hb \cdot H_2O_2$
7	$MetHb + H_2O_2 \rightarrow FerHb + H_2O$	$v_7 = k_7 \cdot MetHb \cdot H_2O_2$
8	$MetHb + cytb5(red) \rightarrow Hb + cytb5(ox)$	$v_8 = k_8 \cdot MetHb \cdot cytb5(red)$
9	$NADH + cytb5(ox) \xrightarrow{cytb5R} NAD^+ + cytb5(red)$	$v_9 = k_9 \cdot cytb5R \frac{NADH}{K_M^{NADH} + NADH} \times \times \frac{cytb5(ox)}{K_M^{cytb5(ox)} + cytb5(ox)}$
10	$FerHb + 2Asc \rightarrow MetHb + DHA + Asc$	$v_{10} = k_{10} \cdot FerHb \cdot Asc$
11	$DHA + 2GSH \xrightarrow{DHAR} Asc + GSSG$	$v_{11} = \frac{k_{13} \cdot DHAR}{1 + \frac{K_{DHA}}{DHA} + \frac{K_{GSH}}{GSH}}$
12	$GSSG + NADPH \xrightarrow{GSHR} NADP^+ + 2GSH$	$v_{12} = \frac{GSHR \cdot GSSG \cdot NADPH}{K_1 \cdot NADPH + K_2 \cdot GSH}$
13	$MetHb + Band3 \rightarrow MetHbcomplex$	$v_{13} = k_{13} \cdot MetHb \cdot Band3$
14	$MetHbcomplex \rightarrow MetHb + Band3$	$v_{14} = k_{14} \cdot MetHbcomplex$
15	$FerHb + Band3 \rightarrow FerHbcomplex$	$v_{15} = k_{15} \cdot FerHb \cdot Band3$
16	$FerHbcomplex \rightarrow FerHb + Band3$	$v_{16} = k_{16} \cdot FerHbcomplex$

is decreased, the equilibrium is violated; this leads to a reverse reaction catalyzed by LDH to restore the balance.

Regulation of the Asc/DHA redox pair is carried out with the participation of the electrons of GSH by dehydroascorbate reductase (DHAR) (v_{11}) [31]. As a result of this reaction, glutathione disulfide (GSSG) is formed, which is reduced by glutathione reductase (GSHR) (v_{12}) with the participation of the electrons from NADPH. NADPH is reduced in the pentose phosphate pathway with the participation of glucose-6-phosphate dehydrogenase (G6PDH) and phosphogluconate dehydrogenase (GO6PDH) [33, 38].

The formation of methemoglobin leads to its interaction with the erythrocyte membrane, namely, binding to the band 3 protein (Band 3) [12, 20]. To simulate this process, the kinetics of ligand-receptor binding was considered [33]. Methemoglobin acts as a ligand, and the membrane Band 3 protein serves as a receptor. The formation of the complex is reversible and is characterized by the constants of formation and decomposition of the complex (v_{13} and v_{14}). Excess of hydrogen peroxide cause the formation of ferrylhemoglobin, which is also able to bind to the membrane of erythrocytes. This process was considered similarly to the previous one with the rates (v_{15} and v_{16}).

The constructed mathematical model was nonlinear and contained 41 differential equations. Considering the dynamics of the process was a fundamentally new approach, which made it possible to study not

Table 2. Parameter values in the model

No	Reaction constants from Table 1	Reference
1	$P = 6 \times 10^{-6}$ m s^{-1} $S_{cell} = 1.09 \times 10^{-10}$ m^2 $V = 10^{-6}$ m^3 $N_{cell} = 3 \times 10^7$	[28, 29]
2	$P = 6 \times 10^{-6}$ m s^{-1} $S_{cell} = 1.09 \times 10^{-10}$ m^2 $V_{cell} = 6.3 \times 10^{-17}$ m^3	[28, 29]
3	$k_3 = 6 \times 10^6$ M^{-1} s^{-1}	[6]
4	$k_4 = 1.6 \times 10^7$ M^{-1} s^{-1}	[6]
5	Gpx $= 1.4 \times 10^{-6}$ M $K_1 = 2.5 \times 10^{-5}$ M s $K_2 = 2.4 \times 10^{-8}$ M s	[7]
6	$k_6 = 100$ M^{-1} s^{-1}	[6]
7	$k_7 = 98$ M^{-1} s^{-1}	[30]
8	$k_8 = 6200$ M^{-1} s^{-1}	[24]
9	$k_9 = 418$ s^{-1} cytb5R $= 7 \times 10^{-8}$ M $K_M^{NADH} = 3.1 \times 10^{-7}$ M $K_M^{cytb5(ox)} = 1.5 \times 10^{-5}$ M	[24]
10	$k_{10} = 400$ M^{-1} s^{-1}	[30]
11	$k_{11} = 5.27$ s^{-1} DHAR $= 10^{-7}$ M $K_{DHA} = 2.1 \times 10^{-4}$ M $K_{GSH} = 3.5 \times 10^{-3}$ M	[31]
12	GSHR $= 1.4 \times 10^{-6}$ M $K_1 = 2.4 \times 10^{-8}$ M s $K_2 = 2.5 \times 10^{-5}$ M s	[7]
13	$k_{13} = 3$ M^{-1} s^{-1}	[12]
14	$k_{14} = 7.8 \times 10^{-5}$ s^{-1}	[12]
15	$k_{15} = 30$ M^{-1} s^{-1}	[21]
16	$k_{16} = 0.8 \times 10^{-5}$ s^{-1}	[21]

Table 3. Initial values of parameters in the model

Reagent designation	Initial value	Reference
H_2O_2 (ext)	$0–2.5 \times 10^{-4}$ M	This study
H_2O_2	0	This study
Cat	5.5×10^{-6} M	[7]
Comp I	5.5×10^{-6} M	[7]
Hb	0.01 M	[24]
MetHb	0	[24]
FerHb	0	[30]
cyt b5(red)	8.12×10^{-7} M	[24]
cyt b5(ox)	0	[24]
NADH	1.48×10^{-7} M	[32]
NAD^+	8.9×10^{-5} M	[32]
Asc	7.5×10^{-5} M	[1]
DHA	0	[1]
GSH	1.5×10^{-3} M	[7]
GSSG	0	[7]
NADPH	5×10^{-5} M	[7]
$NADP^+$	0.2×10^{-6} M	[7]
Band 3	2.6×10^{-5} M	[33]
complex MetHb	0	[12]
complex FerHb	0	[21]

only the amplitudes, but also the duration of the signals. All constants and initial conditions were taken from literature sources. An analysis of the stability of the system was performed. The numerical solution of the system was performed with the Wolfram Mathematica software. The full form of differential equations is presented in the Annex.

Numerical modeling of the processes of interaction of methemoglobin with the erythrocyte membrane made it possible to determine the concentration range of extracellular hydrogen peroxide, at which the activation of adaptive processes would be observed; this allowed experimental verification of the model. The effect of hydrogen peroxide on the structural stability of membranes was studied in the experiments in vitro with erythrocyte hemolysis induced by hypochlorous acid.

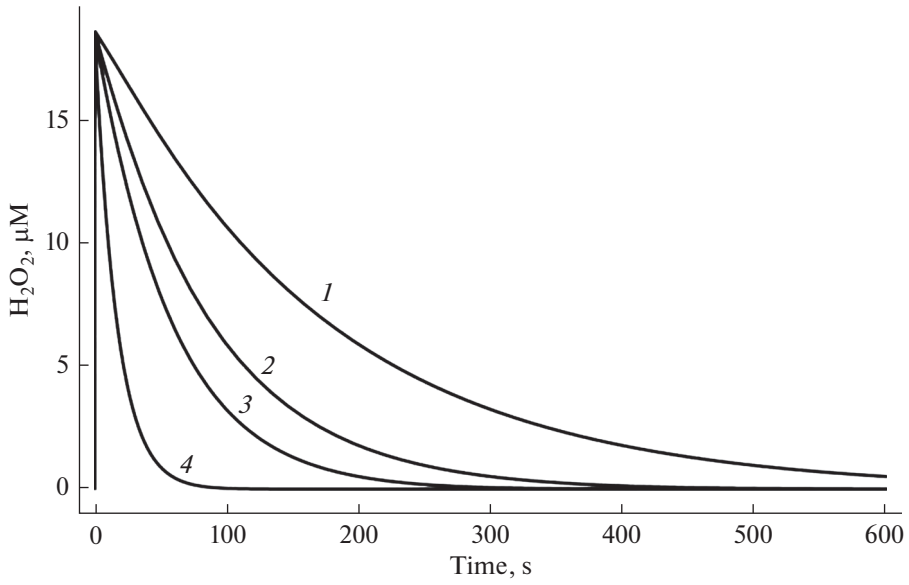

Fig. 2. Kinetics of utilization of intracellular hydrogen peroxide in cuvettes with different number of cells: cuvette (*1*), 1×10^7 cells; cuvette (*2*), 2×10^7 cells; cuvette (*3*), 3×10^7 cells; and cuvette (*4*), 10^8 cells.

MATERIALS AND METHODS

Sodium hypochlorite (NaOCl) (Sigma-Aldrich) and hydrogen peroxide (Belmedpreparaty, Belarus) were used in the experiments.

The concentration of the NaOCl solution was determined spectrophotometrically as the concentration of OCl^- at pH 12.0, which has the molar extinction coefficient (ε_{292}) of 350 M^{-1} cm^{-1}. Since pK_α for HOCl is approximately of 7.5 at physiological pH, half of the compound was present in the protonated form of HOCl and half in the deprotonated form of OCl^-. Thus, HOCl was a mixture of $HOCl/OCL^-$. A working solution of HOCl was prepared immediately before analysis by dissolving the preparation in a 10 mM sodium-phosphate buffer (pH 7.4) containing 137 mM NaCl.

In the experiments, the blood of healthy donors obtained at the Republican Scientific and Practical Center of Transfusiology and Medical Biotechnologies was used. Erythrocytes were isolated and washed by centrifugation at 300 *g* in a phosphate buffered saline (PBS) containing 10 mM Na_2HPO_4/KH_2PO_4, 137 mM NaCl, 2.7 mM KCl, and 5 mM *D*-glucose (pH 7.4).

The kinetics of erythrocyte hemolysis was measured using a Solar CM-2203 spectrofluorimeter (SOLAR, Belarus) by recording the optical density of the cell suspension (3×10^7 cells/mL) at 640 nm. The concentration of erythrocytes was chosen in such a way that the initial optical density was of 0.5, which was optimal for measurements. A 1-mL aliquot of a suspension of washed erythrocytes was added to the optical cuvette and thermostated for 3–4 min at 37°C with constant stirring. Hemolysis was initiated by adding 0.2 mM HOCl to the suspension of erythrocytes in PBS after incubation with H_2O_2 for 5 or 15 min at concentrations of 10–250 μM.

The effect of the treatments (*I*) was evaluated as the relative difference of optical density after 10 min incubation with hypochlorous acid in the presence of hydrogen peroxide and optical density after 10 min incubation with hypochlorous acid without hydrogen peroxide.

The results were presented as mean values with standard deviation of the mean for three to five independent experiments. Statistical analysis was carried out using the Microsoft Excel software. The statistical significance of the difference between mean values was assessed using the Student's *t*-test, the significance level was taken as $p < 0.05$.

RESULTS AND DISCUSSION

The proposed model made it possible to calculate the dynamics of intracellular signaling processes involving methemoglobin and ferrylhemoglobin depending on the extracellular concentration of hydrogen peroxide. Numerical experiments based on the constructed model gave the following results.

Owing to diffusion and the action of catalase, a rapid (approximately for a second) establishment of the gradient of H_2O_2 concentrations on the plasma membrane is generated. The intracellular concentra-

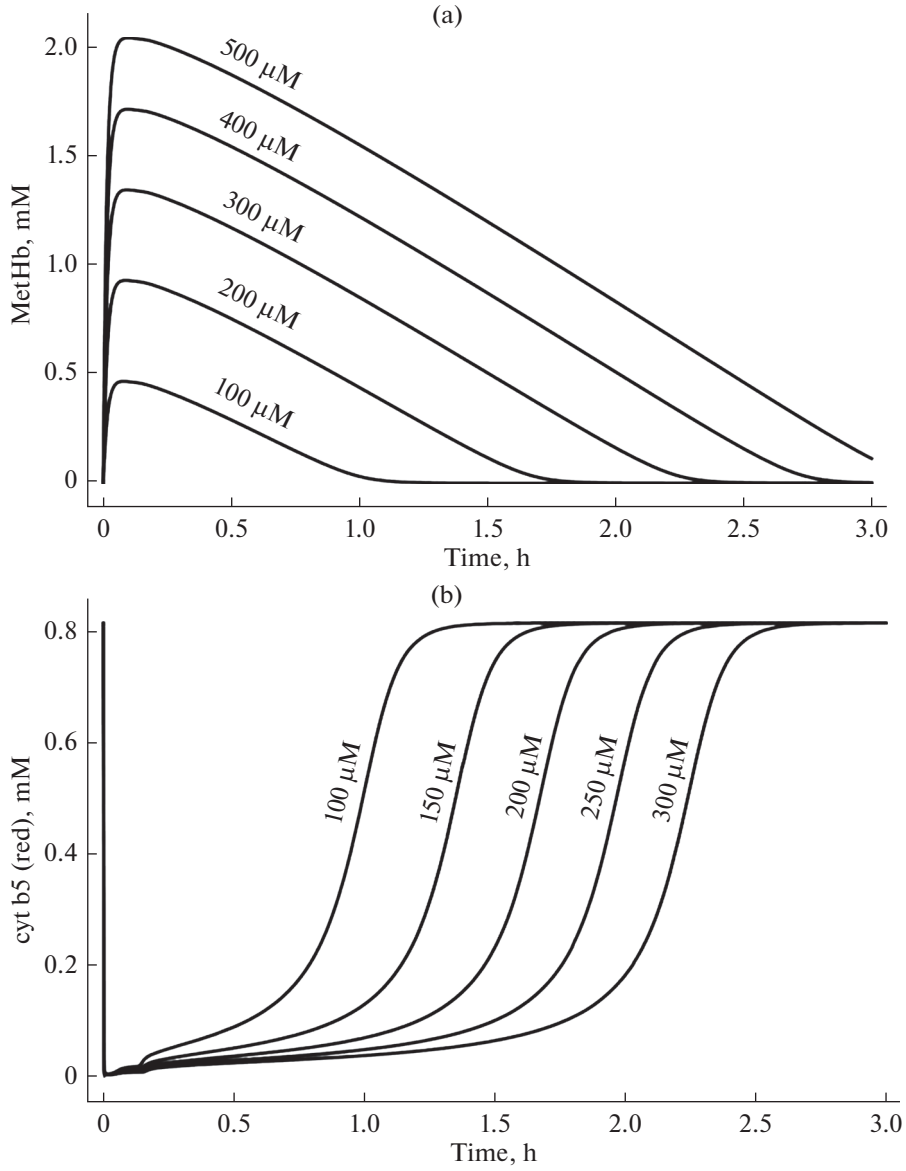

Fig. 3. Kinetics of formation and reduction of methemoglobin (MetHb) (a) and cytochrome b5 (red) (b) at different concentrations of extracellular hydrogen peroxide.

tion of hydrogen peroxide depends on the extracellular concentration, which decreases because of utilization of the H_2O_2 by the cells. Utilization, and consequently, the dynamics of changes in extracellular and intracellular concentrations of hydrogen peroxide is proportional to the number of cells in the sample. Figure 2 shows the dynamics of intracellular hydrogen peroxide at an extracellular concentration of 200 μM and at different number of erythrocytes in the sample. The consequence of the utilization of the oxidant is an exponential decrease in its intracellular and extracellular concentration. Figure 2 also shows that at a concentration of about 200 μM and a cell count of 3×10^7, the total duration of the hydrogen peroxide signal does not exceed 300 s, and the intracellular concentration does not exceed 10% of the extracellular concentration, which is consistent with the data obtained in [23].

An increase in the intracellular concentration of hydrogen peroxide leads to an increase in the formation of methemoglobin (Fig. 3a), concentration of which reaches 2–3 mM. The obtained results were confirmed by the experimental studies [39]. Methemoglobin induces membrane stabilization and an increase in structural stability by forming complexes with cytoskeleton proteins [9, 40]. A decrease in the concentration of methemoglobin owing to its reduc-

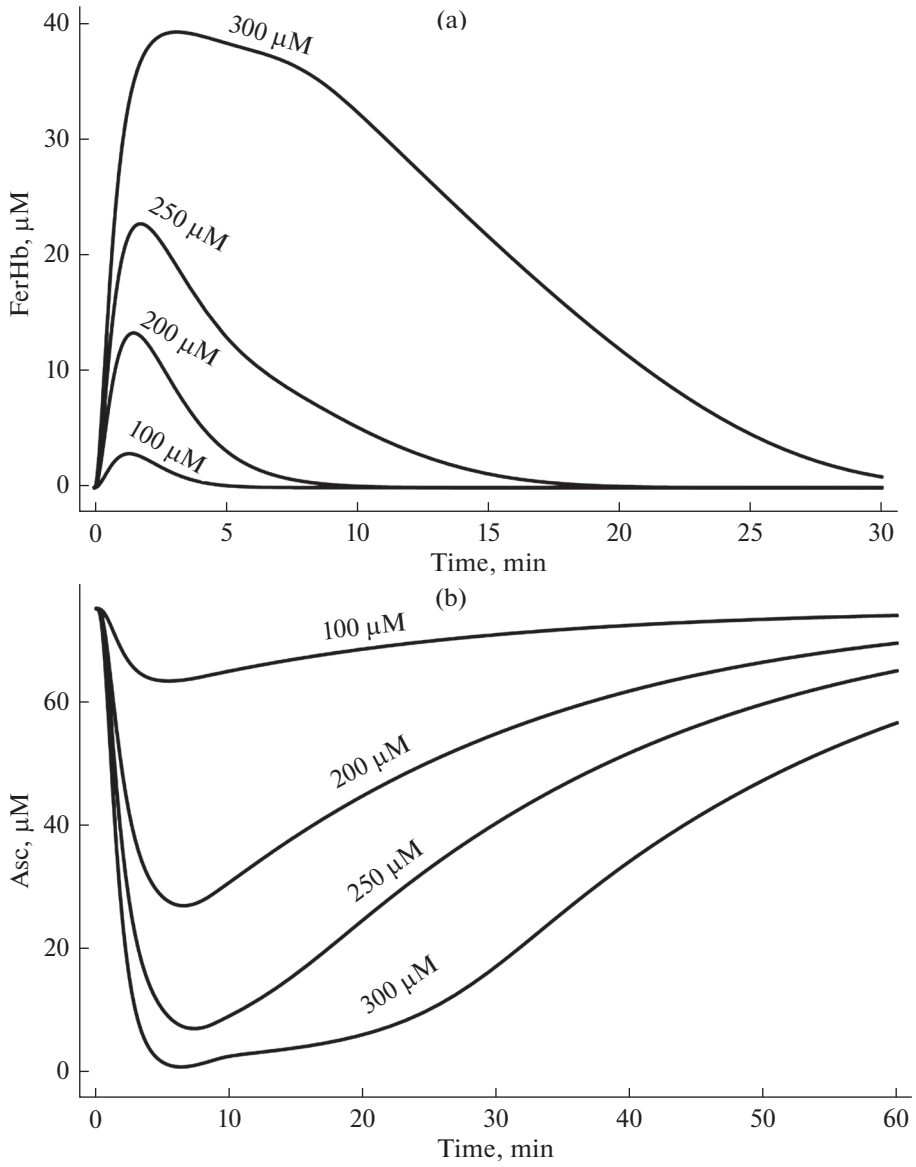

Fig. 4. Kinetics of formation and reduction of ferrylhemoglobin (FerHB) (a) and ascorbate (b) at different concentrations of extracellular hydrogen peroxide.

tion by cytochrome b5 leads to the breakdown of its membrane complexes. In the model, the total reduction time of methemoglobin for the H_2O_2 concentrations of 200–300 μM is 2–3 h, which is comparable to the time presented in [39]. The dynamics of changes in the concentration of cytochrome b5 used for the reduction of oxidized hemoglobin depends on the concentration of H_2O_2; at the H_2O_2 concentrations exceeding 100 μM, the amount of reduced protein decreases to zero, which increases the time of reduction of methemoglobin (Fig. 3b). An increase in the rate of NADH reduction with an increase in extracellular lactate concentration (which can be observed with muscle exertion, hypoxia, and various pathological processes) will accelerate the process of methemoglobin reduction.

A further increase in the concentration of extracellular H_2O_2 leads to the oxidation of methemoglobin and the formation of ferrylhemoglobin, which can also bind to the cell membrane. The amount of ferrylhemoglobin formed depends on the amount of hydrogen peroxide that entered the cells and the amount of methemoglobin formed. The paper [41] presented experimental data on the amount of ferrylhemoglobin at the ratio $[H_2O_2]$: [MetHb] = 10 : 1 and indicated complete oxidation of methemoglobin. In our experiments, this ratio did not rise above 1 : 1 and the model

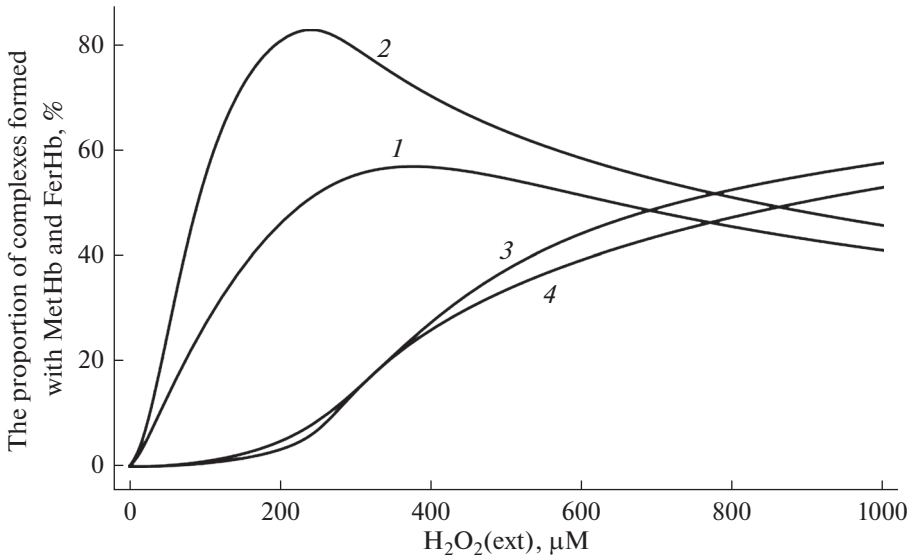

Fig. 5. The proportion of methemoglobin–membrane complexes formed after 5-min (*1*) and 15-min (*2*) pre-incubation and the proportion of ferrylhemoglobin–membrane complexes after 5-min (*3*) and 15-min (*4*) pre-incubation depending on the concentration of extracellular hydrogen peroxide.

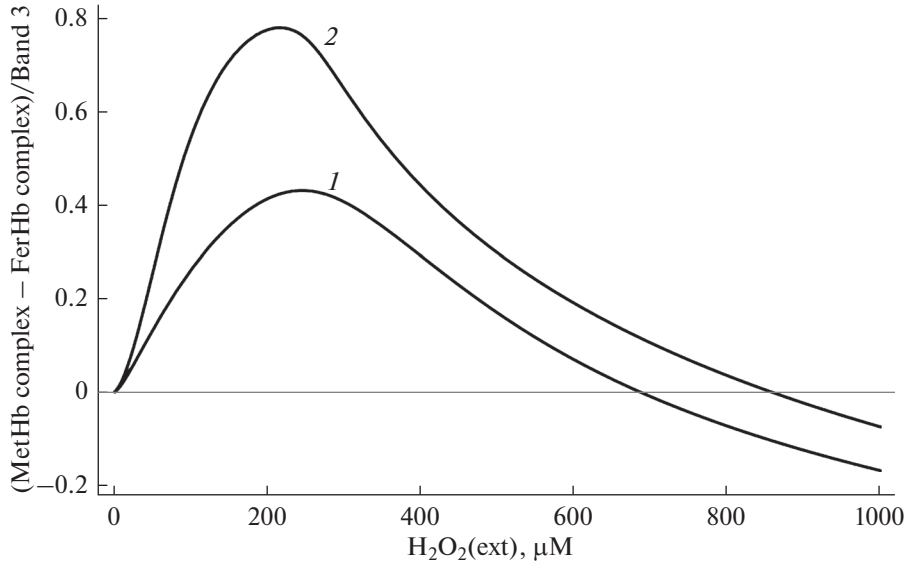

Fig. 6. Relative difference in the number of methemoglobin–membrane and ferrylhemoglobin–membrane complexes formed at different concentrations of extracellular hydrogen peroxide after 5-min (*1*) and 15-min (*2*) pre-incubation.

predicted the oxidation of 5% methemoglobin. The formation of a ferrylhemoglobin complex with the erythrocyte membrane disrupts interaction of cytoskeleton with the membrane, which leads to a decrease in the structural stability of the cell [21]. Figure 4a shows the dependence of the amount of ferrylhemoglobin formed on the concentration of extracellular hydrogen peroxide. Upon reaching 250 μM of H_2O_2, an increase in the intensity of ferrylhemoglobin formation is observed, which is associated with depletion of the intracellular ascorbate pool (Fig. 4b). The model considering glycolysis shows that there would be a slowdown in the formation of NADH and NADPH under hypoglycemia, which leads to the

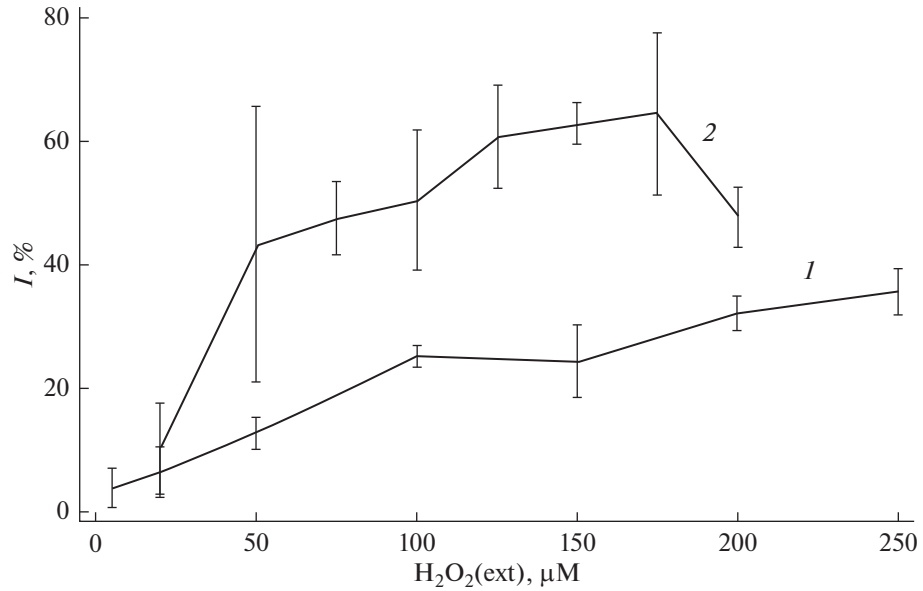

Fig. 7. The proportion of non-hemolysed erythrocytes depending on the concentration of extracellular hydrogen peroxide after 5-min (*1*) and 15-min (*2*) pre-incubation.

accumulation of oxidized forms of hemoglobin and an increase in the number of ferrylhemoglobin membrane complexes.

Within the framework of the proposed model of the adaptive mechanism, the degree of increase in the structural stability of the membrane depends on the number of membrane–methemoglobin and membrane–ferrylhemoglobin complexes formed. The proportion of receptors occupied by one or another protein, in turn, depends on the extracellular concentration of hydrogen peroxide and the incubation time. Figure 5 shows the theoretically calculated dependences of the fraction of the formed membrane complexes of proteins on the extracellular concentration of hydrogen peroxide. The dependence of the relative difference in the number of membrane–methemoglobin and membrane–ferrylhemoglobin complexes on the concentration of H_2O_2 was bell-shaped (Fig. 6). At concentrations of hydrogen peroxide below 200 μM, an increase in the number of complexes with methemoglobin is observed in the cell with an increase in concentration. An increase in the incubation time from 5 to 15 min also leads to an increase in the number of membrane complexes formed by methemoglobin. At higher concentrations of the oxidant, the proportion of membrane complexes formed with methemoglobin decreases. Exceeding the concentration of 200 μM induces a sharp increase in the number of ferrylhemoglobin–membrane complexes, which is associated with a decrease in the number of reducing agent molecules. When the H_2O_2 concentration reaches 800 μM, the number of complexes becomes equal. Thus, according to this model, under the action of extracellular H_2O_2 at concentrations from 10 to 200 μM, a dose–dependent increase in the number of membrane-methemoglobin complexes, and consequently, an increase in the structural stability of the membrane is observed.

In the experimental study of the rate of erythrocyte hemolysis, it has been shown that pre-incubation of the cells with hydrogen peroxide at concentrations of 10–200 μM indeed reduced the proportion of hemolysed erythrocytes. The maximum protective effect, as predicted by the model (Fig. 6), depends on the incubation time of the cells with H_2O_2. Figure 7 shows the dependences of the proportion of unaffected erythrocytes on the extracellular concentration of hydrogen peroxide for incubation times of 5 and 15 min. With preliminary incubation of the cells for 5 min, a stabilizing effect was observed, reaching 30% of the control values. When the cells were incubated with hydrogen peroxide for 15 min, a more pronounced stabilizing effect was observed: the proportion of unaffected erythrocytes reached 60% for hydrogen peroxide at a concentration of 175 μM. However, at higher concentrations, the inverse relationship was manifested: with an increase in the concentration of H_2O_2, the proportion of unaffected erythrocytes decreased, which was probably due to an increase in the number of ferrylhemoglobin–membrane complexes. An increase in the number of these complexes could initiate the processes of lipid peroxidation and disrupt the interaction of the cytoskeleton with the membrane, which would

lead to a decrease of the structural stabilization effect at high concentrations of H_2O_2.

CONCLUSIONS

The construction of an adequate mathematical model of the adaptation mechanism of erythrocytes contributes to the analysis of optimal conditions for its regulation by external factors. In this study, a mathematical model has been constructed that considers the contribution of various participants in hemoglobin metabolism to the regulation of the structural stability of the membrane. The results of numerical modeling showed that reversible binding of methemoglobin to the membrane can be an adaptive mechanism aimed at stabilizing the lipid bilayer of the membrane. On the other hand, an increase in the concentration of an oxidized form of hemoglobin, ferylhemoglobin, and its binding to the membrane can lead to an increase in pathophysiological processes (lipid peroxidation, disruption of the interaction of the membrane with the cytoskeleton, etc.), which can reduce the structural stability of the cells. Apparently, the ratio of membrane complexes of various oxidized forms of hemoglobin determines the hormesis dependence of the response of erythrocytes to the action of hydrogen peroxide, that is, regulatory at low concentrations and damaging at high concentrations. To analyze optimal conditions, the model considered the extracellular concentration of hydrogen peroxide, the number of cells in the sample, the state of the erythrocyte antioxidant system (the content of ascorbate and other reducing agents), the metabolic activity of cells (glycolysis and pentose phosphate pathway), and external metabolic conditions (lactate content). As a result of theoretical and experimental studies, it has been shown that under the action of hydrogen peroxide at concentrations of 10–200 μM, the adaptive mechanism of erythrocytes was activated due to an increase in the number of membrane-bound methemoglobin, which increased the structural stability of the membrane under oxidative stress. The obtained data expand the understanding of the mechanisms of protection of erythrocytes and make it possible to predict the protective properties of the cells under oxidative stress.

ACKNOWLEDGMENTS

The work was partially supported by the Belarusian Republican Foundation for Basic Research (project no. B20U-1).

COMPLIANCE WITH ETHICAL STANDARDS

The authors declare that they have no conflict of interest.

All procedures performed in studies involving human participants were in accordance with the ethical standards of the 1964 Helsinki Declaration and its later amendments or comparable ethical standards. Informed consent was obtained from all individual participants involved in the study.

REFERENCES

1. Martinovich G.G., Cherenkevich S.N. 2008. *Okislitel-no-vosstanovitelnie processi v kletkah* (Redox processes in cells). Minsk: BSU.
2. Sies H., Jones D.P. 2020. Reactive oxygen species (ROS) as pleiotropic physiological signalling agents. *Nat. Rev. Mol. Cell Biol.* **21** (3), 1–21.
3. Ghezzi P., Jaquet V., Marcucci F., Schmidt H. 2017. The oxidative stress theory of disease: Levels of evidence and epistemological aspects. *Br. J. Pharmacol.* **174**, 1784–1796.
4. Ursini F., Maiorino M., Forman H.J. 2016. Redox homeostasis: The golden mean of healthy living. *Redox Biology*. **8**, 205–215.
5. Lim J.B., Huang B.K., Deen W.M., Sikes H.D. 2015. Analysis of the lifetime and spatial localization of hydrogen peroxide generated in the cytosol using a reduced kinetic model. *Free Radic. Biol. Med.* **89**, 47–53.
6. Johnson R.M., Goyette G.Jr., Ravindranath Y., Ho Y. 2005. Hemoglobin autoxidation and regulation of endogenous H_2O_2 levels in erythrocytes. *Free Radic. Biol. Med.* **39**, 1407–1417.
7. Orrico F., Möller M.N., Cassina A., Denicola A., Thomson L. 2018. Kinetic and stoichiometric constraints determine the pathway of H_2O_2 consumption by red blood cells. *Free Radic. Biol. Med.* **121**, 231–239.
8. Merry T.L., Ristow M. 2016. Mitohormesis in exercise training. *Free Radic. Biol. Med.* **98**, 123–130. https://doi.org/10.1016/j.freeradbiomed.2015.11.032
9. Kosmachevskaya O.V., Nasybullina E.I., Blindar V.N., Topunov A.F. 2019. Binding of erythrocyte hemoglobin to the membrane as a way of implementing the signal-regulatory function (review). *Applied Biochem. Microbiol.* **55** (2), 83–98.
10. Zenkov N.K., Chechushkov A.V., Kozhin P.M., Kandalintseva N.V., Martinovich G.G., Menshchikova E.B. 2017. Mazes of Nrf2 Regulation. *Biochemistry (Moscow)*. **82** (5), 556–564.
11. Cuadrado A., Rojo A., Wells G., Hayes J., Cousin S., Rumsey W., Attucks O., Franklin S., Levonen A., Kensler T., Dinkova-Kostova A. 2019. Therapeutic targeting of the NRF2 and KEAP1 partnership in chronic diseases. *Nat. Rev. Drug Discov.* **18,** 295–317.
12. Arashiki N., Kimata N., Manno S., Mohandas N., Takakuwa Y. 2013. Membrane peroxidation and methemoglobin formation are both necessary for band 3 clustering: Mechanistic insights into human erythrocyte senescence. *Biochemistry.* **52**, 5760–5769.
13. Kuhn V., Diederich L., Stevenson Keller IV T.C., Kramer C.M., Lückstädt W., Panknin C., Suvorava T., Isakson B.E., Kelm M., Cortese-Krott M.M. 2017. Red blood cell function and dysfunction: Redox regulation,

nitric oxide metabolism, anemia. *Antioxid. Redox Signal.* **26** (13), 718–742.

14. Forman H.J., Bernardo A., Davies K.J.A. 2016. What is the concentration of hydrogen peroxide in blood and plasma? *Arch. Biochem. Biophys.* **603,** 48–53.
15. Roy S., Khanna S., Nallu K., Hunt T.K., Sen C.K. 2006. Dermal wound healing is subject to redox control. *Mol. Ther.* **13** (1), 211–220.
16. Niethammer P., Grabher C., Look A.T., Mitchison T.J. 2009. A tissue-scale gradient of hydrogen peroxide mediates rapid wound detection in zebrafish. *Nature.* **459** (7249), 996–999.
17. Zavodnik I.B., Lapshina E.A., Zavodnik L.B., Soszynski M., Bartosz G., Bryszewska M. 2002. Hypochlorous acid-induced oxidative damage of human red blood cells: Effects of tert-butyl hydroperoxide and nitrite on the HOCl reaction with erythrocytes. *Bioelectrochemistry*. **58**, 127–135.
18. Liu S., Palek J. 1984. Hemoglobin enhances the self-association of spectrin heterodimers in human erythrocytes. *J. Biol. Chem*. **259** (18), 11556–11562.
19. Snyder L.M., Fortier N.L., Trainor J., Jacobs J., Lob L., Lubin B., Chiu D., Shohet S., Mohandas N. 1985. Effect of hydrogen peroxide exposure on normal human erythrocyte deformability, morphology, surface characteristics, and spectrin-hemoglobin cross-linking. *J. Clin. Invest.* **76**, 1971–1977.
20. Kaul R.K., Köhler H. 1983. Interaction of hemoglobin with Band 3: A review. *Klin. Wochenschr*. **61**, 831–837.
21. Welbourn E.M., Wilson M.T., Yusof A., Metodiev M.V., Cooper C.E. 2017. The mechanism of formation, structure, and physiological relevance of covalent hemoglobin attachment to the erythrocyte membrane. *Free Radic. Biol. Med.* **103**, 95–106.
22. Jarolim P., Lahav M., Liu S.C., Palek J. 1990. Effect of hemoglobin oxidation products on the stability of red cell membrane skeletons and the associations of skeletal proteins: Correlation with a release of hemin. *Blood.* **76**. 2125–2131
23. Nicholls P. 1965. Activity of catalase in the red cell. *Biochim. Biophys. Acta.* **99**, 286–297.
24. Kinoshita A., Nakayama Y., Kitayama T., Tomita M. 2007. Simulation study of methemoglobin reduction in erythrocytes. Differential contributions of two pathways to tolerance to oxidative stress. *FEBS J.* **274**, 1449–1458.
25. Rapoport T.A., Heinrich R., Jacobasch G., Rapoport S. 1974. A linear steady-state treatment of enzymatic chains. A mathematical model of glycolysis of human erythrocytes. *Eur. J. Biochem.* **42**, 107–120.
26. Ataullakhanov F.I., Vitvitsky V.M., Jabotinsky A.M., 1977. Quantitative model of human erythrocytes glycolysis. Biofizika (Rus.). **22** (3), 483–488.
27. Mulquiney P.J., Kuchel P.W. 1999. Model of 2,3-bisphosphoglycerate metabolism in the human erythrocyte based on detailed enzyme kinetic equations: Equations and parameter refinement. *Biochem. J.* **342**, 581–596.
28. Martinovich G.G., Cherenkevich S.N. 2005. Consumption of intracellular hydrogen peroxide in epithelial human amnion cells. *Biomeditsinskaya Khimiya (Rus.)*. **51** (6), 626–633.
29. Lipunova E.A., Skorkina M.Yu. 2004. *Sistema krasnoy krovi: Sravnitelnaya fiziologoya* (The red blood system: Comparative physiology). Belgorod: BelSU Publishing House.
30. Gebicka L., Banasiak E. 2009 Flavonoids as reductants of ferryl hemoglobin. *Acta Biochim. Pol.* **56** (3) 509–513.
31. Peng Xu D., Washburn M.P., Ping Sun G. Wells W. 1996. Purification and characterization of a glutathione dependent dehydroascorbate reductase from human erythrocytes. Biochem. Biophys. Res. Commun. **221** (1), 117–121.
32. Bali M., Thomas S.R. 2001. A modelling study of feedforward activation in human erythrocyte glycolysis. *C.R. Acad. Sci. III.* **324**, 185–199.
33. Cherenkevich S.N., Martinovich G.G., Khmelnitsky A.I. 2008. *Biologicheskie membrany* (Biological membranes). Minsk: BSU.
34. Miłek J. 2018. Estimation of the kinetic parameters for H_2O_2 enzymatic decomposition and for catalase deactivation. *Braz. J. Chem. Eng.* **35** (3), 995–1004.
35. Benfeitas R., Selvaggio G., Antunes F., Coelho P.M.B.M., Salvador A. 2014. Hydrogen peroxide metabolism and sensing in human erythrocytes: A validated kinetic model and reappraisal of the role of peroxiredoxin II. *Free Radic. Biol. Med.* **74**, 35–49.
36. Kanias T., Acker J.P. 2010. Biopreservation of red blood cells – the struggle with hemoglobin oxidation. *FEBS J.* **277**, 343–356.
37. May J.M., Qu Z., Cobb C.E. 2004. Human erythrocyte recycling of ascorbic acid. *J. Biol. Chem.* **279** (15), 14975–14982.
38. Martinovich G.G., Sazanov L.A., Cherenkevich S.N. 2017. *Kletochnaya bioenergetika: Fiziko-khimicheskie i molekularnie osnovy* (Cellular bioenergetics: Physicochemical and molecular basis). M.: LENAND.
39. Jaffe E.R. 1963. The reduction of methemoglobin in erythrocytes of a patient with congenital methemoglobinemia, subjects with erythrocyte glucose-6-phosphate dehydrogenase deficiency, and normal individuals. *Blood.* **21** (5), 561–572.
40. Mendanha S.A., Anjos J.L.V., Silva A.H.M., Alonso A. 2012. Electron paramagnetic resonance study of lipid and protein membrane components of erythrocytes oxidized with hydrogen peroxide. *Braz. J. Med. Biol. Res.* **45**, 473–481.
41. Kassa T., Jana S., Meng F., Alayash A.I. 2016. Differential heme release from various hemoglobin redox states and the upregulation of cellular heme oxygenase-1. *FEBS Open Bio.* **6**, 876–884.

Translated by E. Puchkov

APPENDIX

The system of differential equations used in this study is presented below. In this form, the system was presented in the Wolfram Mathematica software.

$glc'[t] = vGLUT - vHK$	$glc[0] = 5 \times 10^{-3}$
$g6p'[t] = vHK - vPGI - vG6PDH$	$g6p[0] = 6 \times 10^{-5}$
$f6p'[t] = vPGI - vPFK + vTA + vTK2$	$f6p[0] = 1.9 \times 10^{-5}$
$fdp'[t] = vPFK - vALD$	$fdp[0] = 5.6 \times 10^{-6}$
$dhap'[t] = vALD - vTPI$	$dhap[0] = 1.5 \times 10^{-5}$
$ga3p'[t] = vALD + vTPI - vGAPDH - vTA + vTK1 + vTK2$	$ga3p[0] = 3.6 \times 10^{-6}$
$b13pg'[t] = vGAPDH - vPGK$	$b13pg[0] = 2.3 \times 10^{-7}$
$p3g'[t] = vPGK - vPGM$	$p3g[0] = 4.8 \times 10^{-5}$
$p2g'[t] = vPGM - vEN$	$p2g[0] = 1.4 \times 10^{-5}$
$pep'[t] = vEN - vPK$	$pep[0] = 8.1 \times 10^{-6}$
$pyr'[t] = vPK - vLDH - vpyrtr$	$pyr[0] = 5.2 \times 10^{-5}$
$lac'[t] = vLDH - vlactr$	$lac[0] = 1.3 \times 10^{-3}$
$ATP'[t] = -vHK - vPFK + vPGK + vPK$	$ATP[0] = 1.4 \times 10^{-3}$
$ADP'[t] = vHK + vPFK - vPGK - vPK$	$ADP[0] = 1.5 \times 10^{-4}$
$gl6p'[t] = vG6PDH - vPGLase$	$gl6p[0] = 3.6 \times 10^{-4}$
$go6p'[t] = vPGLase - v6PGODH$	$go6p[0] = 4.5 \times 10^{-5}$
$ru5p'[t] = v6PGODH - vX5PI - vR5PI$	$ru5p[0] = 4.9 \times 10^{-6}$
$x5p'[t] = vX5PI - vTK1 - vTK2$	$x5p[0] = 9 \times 10^{-6}$
$r5p'[t] = vR5PI - vTK1$	$r5p[0] = 5.8 \times 10^{-6}$
$s7p'[t] = vTK1 - vTA$	$s7p[0] = 2.1 \times 10^{-5}$
$e4p'[t] = vTA - vTK2$	$e4p[0] = 4.5 \times 10^{-7}$
$Cat1'[t] = -v3 + v4$	$Cat1[0] = 5.5 \times 10^{-6}$
$Cat2'[t] = v3 - v4$	$Cat2[0] = 5.5 \times 10^{-6}$
$H2O2ex'[t] = -v1$	$H2O2ex[0] = (1 \ldots 250) \times 10^{-6}$
$H2O2'[t] = v2 - v3 - v4 - v5 - v6 - v7$	$H2O2[0] = 0$
$cytb5r'[t] = -v8 + v9$	$cytb5r[0] = 8.1 \times 10^{-6}$
$cytb5ox'[t] = v8 - v9$	$cytb5ox[0] = 0$
$metHb'[t] = v6 - v7 - v8 - v13 + v10 + v14$	$metHb[0] = 0$
$ferHb'[t] = v7 - v10 - v15 + v16$	$ferHb[0] = 0$
$metHbcomplex'[t] = v13 - v14$	$metHbcomplex[0] = 0$
$ferHbcomplex'[t] = v15 - v16$	$ferHbcomplex[0] = 0$
$B3'[t] = -v13 + v14 - v15 + v16$	$B3[0] = 2.6 \times 10^{-5}$
$Hb'[t] = -v6 + v8$	$Hb[0] = 0.01$
$Asc'[t] = -v10 + v11$	$Asc[0] = 7.5 \times 10^{-5}$
$DHA'[t] = v10 - v11$	$DHA[0] = 0$
$GSH'[t] = 2 \times (-v5 - v11 + v12)$	$GSH[0] = 1.5 \times 10^{-3}$
$GSSG'[t] = v5 + v11 - v12$	$GSSG[0] = 0$
$NADP'[t] = -vG6PDH - v6PGODH + v12$	$NADP[0] = 0.2 \times 10^{-6}$
$NADPH'[t] = vG6PDH + v6PGODH - v12$	$NADPH[0] = 5 \times 10^{-5}$
$NAD'[t] = -vGAPDH + vLDH - v9$	$NAD[0] = 8.9 \times 10^{-5}$
$NADH'[t] = vGAPDH - vLDH + v9$	$NADH[0] = 1.5 \times 10^{-7}$

$$\mathbf{vGLUT} = \frac{\frac{0.0207}{1.7\times10^{-3}}\times(\mathrm{glcex}-\mathrm{glc[t]})}{1+\frac{\mathrm{glcex}}{1.7\times10^{-3}}+\frac{\mathrm{glc[t]}}{6.9\times10^{-3}}+0.54\times\frac{\mathrm{glcex}\times\mathrm{glc[t]}}{1.7\times6.9\times10^{-6}}};\ \mathbf{vPGI} = 2.18\times10^{-7}\times\frac{\frac{1470\times\mathrm{g6p[t]}}{1.81\times10^{-4}}-\frac{1760\times\mathrm{f6p[t]}}{7.1\times10^{-5}}}{1+\frac{\mathrm{g6p[t]}}{1.81\times10^{-4}}+\frac{\mathrm{f6p[t]}}{7.1\times10^{-5}}};\ \mathbf{vTPI} = 1.14\times10^{-6}\times\frac{\frac{1280\times\mathrm{dhap[t]}}{1.62\times10^{-4}}-\frac{14560\times\mathrm{ga3p[t]}}{4.46\times10^{-4}}}{1+\frac{\mathrm{dhap[t]}}{1.62\times10^{-4}}+\frac{\mathrm{ga3p[t]}}{4.46\times10^{-4}}}$$

$$\mathbf{vHK} = 2.4\times10^{-8}\times\frac{\frac{180\times\mathrm{ATP[t]}\times\mathrm{glc[t]}}{4.7\times10^{-5}\times10^{-3}}-\frac{1.16\times\mathrm{g6p[t]}\times\mathrm{ADP[t]}}{10^{-3}\times4.7\times10^{-5}}}{1+\frac{\mathrm{ATP[t]}}{10^{-3}}+\frac{\mathrm{glc[t]}}{4.7\times10^{-5}}+\frac{\mathrm{g6p[t]}}{4.7\times10^{-5}}+\frac{\mathrm{ADP[t]}}{10^{-3}}+\frac{\mathrm{ATP[t]}\times\mathrm{glc[t]}}{10^{-3}\times4.7\times10^{-5}}+\frac{\mathrm{g6p[t]}\times\mathrm{ADP[t]}}{10^{-3}\times4.7\times10^{-5}}};$$

$$\mathbf{vPFK} = 1.1\times10^{-7}\times\frac{\frac{822\times\mathrm{ATP[t]}\times\mathrm{f6p[t]}}{6.8\times10^{-5}\times2.7\times10^{-4}}-\frac{36\times\mathrm{fdp[t]}\times\mathrm{ADP[t]}}{4.2\times10^{-4}\times5.4\times10^{-4}}}{1+\frac{\mathrm{ATP[t]}}{6.8\times10^{-5}}+\frac{\mathrm{f6p[t]}}{2.7\times10^{-4}}+\frac{\mathrm{fdp[t]}}{6.8\times10^{-5}\times2.7\times10^{-4}}+\frac{\mathrm{ADP[t]}}{4.2\times10^{-4}}+\frac{\mathrm{fdp[t]}\times\mathrm{ADP[t]}}{5.4\times10^{-4}\times4.2\times10^{-4}}};$$

$$\mathbf{vALD} = \frac{\frac{\mathrm{b23pg}}{0.0015}+\frac{\mathrm{fdp[t]}}{1.65\times10^{-5}}+\frac{3.5\times10^{-5}\times\mathrm{ga3p[t]}}{1.9\times10^{-4}\times1.1\times10^{-5}}+\frac{\mathrm{dhap[t]}}{1.1\times10^{-5}}+\frac{3.5\times10^{-5}\times\mathrm{fdp[t]}\times\mathrm{ga3p[t]}}{1.98\times10^{-5}\times1.1\times10^{-5}\times1.9\times10^{-4}}+\frac{\mathrm{ga3p[t]}\times\mathrm{dhap[t]}}{1.1\times10^{-5}\times1.9\times10^{-4}}}{1+\frac{1280\times\mathrm{dhap[t]}}{1.62\times10^{-4}}+\frac{14560\times\mathrm{ga3p[t]}}{4.46\times10^{-4}}+\frac{795\times\mathrm{p3g[t]}}{1.65\times10^{-5}}+\frac{714\times\mathrm{p2g[t]}}{4.6\times10^{-5}}+\frac{190\times\mathrm{p2g[t]}}{1.4\times10^{-4}}+\frac{50\times\mathrm{pep[t]}}{3.1\times10^{-4}}};$$

$$\mathbf{vTPI} = 1.14\times10^{-6}\times\frac{\frac{\mathrm{dhap[t]}}{1.62\times10^{-4}}-\frac{\mathrm{ga3p[t]}}{4.46\times10^{-4}}}{1+\frac{\mathrm{dhap[t]}}{1.62\times10^{-4}}+\frac{\mathrm{ga3p[t]}}{4.46\times10^{-4}}};\ \mathbf{vPGM} = 4.1\times10^{-7}\times\frac{1.68\times10^{-4}-\frac{4.6\times10^{-5}}{3.7\times10^{-7}\times\left(\frac{68\times\mathrm{fdp[t]}}{1.65\times10^{-5}}-\frac{234\times\mathrm{ga3p[t]}\times\mathrm{dhap[t]}}{1.1\times10^{-5}\times1.9\times10^{-4}}\right)}}{1+\frac{\mathrm{p3g[t]}}{1.68\times10^{-4}}+\frac{\mathrm{p2g[t]}}{4.6\times10^{-5}}};\ \mathbf{vEN} = 2.2\times10^{-7}\times\frac{\frac{1.4\times10^{-4}}{\mathrm{p2g[t]}}-\frac{3.1\times10^{-4}}{\mathrm{pep[t]}}}{1+\frac{\mathrm{p2g[t]}}{1.4\times10^{-4}}+\frac{\mathrm{pep[t]}}{3.1\times10^{-4}}}$$

$$\mathbf{vGAPDH} = 7.66\times10^{-6}\times\frac{\frac{\mathrm{ga3p[t]}}{3.1\times10^{-5}}+\left(\frac{\mathrm{b13pg[t]}}{10^{-5}}\right)\times\left(1+\frac{\mathrm{ga3p[t]}}{3.1\times10^{-5}}\right)+\frac{6.7\times10^{-7}\times\mathrm{NADH[t]}}{10^{-5}\times3.3\times10^{-6}}+\frac{9.5\times10^{-5}\times\mathrm{NAD[t]}}{4.5\times10^{-5}\times0.00316}+\frac{\mathrm{NAD[t]}\times\mathrm{ga3p[t]}}{4.5\times10^{-5}\times0.065}+\left(\frac{\mathrm{ga3p[t]}}{0.065}\right)\times\left(1+\frac{\mathrm{ga3p[t]}}{3.1\times10^{-5}}\right)+\frac{\mathrm{NAD[t]}\times\mathrm{b13pg[t]}}{2290\times\mathrm{b13pg[t]}\times\mathrm{ADP[t]}}+\frac{6.7\times10^{-7}\times\mathrm{NADH[t]}}{10^{-5}\times3.3\times10^{-6}}+\frac{\mathrm{ga3p[t]}\times\mathrm{NADH[t]}}{0.065\times10^{-5}}}{1+\frac{232\times\mathrm{NAD[t]}\times\mathrm{ga3p[t]}}{4.5\times10^{-5}\times0.065}-\frac{458\times\mathrm{NADH[t]}\times\mathrm{pyr[t]}}{10^{-5}\times3.3\times10^{-6}}-\frac{115\times\mathrm{NAD[t]}\times\mathrm{lac[t]}}{2765\times\mathrm{b13pg[t]}\times\mathrm{NADH[t]}}};$$

$$\mathbf{vPGK} = 2.74\times10^{-6}\times\frac{\frac{\mathrm{b13pg[t]}}{1.6\times10^{-6}}+\frac{\mathrm{ADP[t]}}{8\times10^{-5}}+\frac{\mathrm{b13pg[t]}\times\mathrm{ADP[t]}}{8\times10^{-5}\times2\times10^{-6}}+\frac{\mathrm{p3g[t]}}{2.05\times10^{-4}}+\frac{\mathrm{ATP[t]}}{1.3\times10^{-4}}+\frac{\mathrm{p3g[t]}\times\mathrm{ATP[t]}}{1.3\times10^{-4}\times0.0011}}{1+\frac{2\times10^{-6}\times8\times10^{-5}}{2\times10^{-6}\times8\times10^{-5}}-\frac{0.0011\times1.3\times10^{-4}}{4.74\times10^{-4}\times2.25\times10^{-4}}-\frac{0.002\times0.003}{1386\times\mathrm{ADP[t]}\times\mathrm{pep[t]}}-\frac{3.26\times\mathrm{pyr[t]}\times\mathrm{ATP[t]}}{4.74\times10^{-4}\times2.25\times10^{-4}}};$$

$$\mathbf{vPK} = 8.7\times10^{-8}\times\frac{\frac{\mathrm{ADP[t]}}{4.74\times10^{-4}}+\frac{\mathrm{pep[t]}}{2.25\times10^{-4}}+\frac{\mathrm{ADP[t]}\times\mathrm{pep[t]}}{4.74\times10^{-4}\times2.25\times10^{-4}}+\frac{\mathrm{pyr[t]}}{0.002}+\frac{\mathrm{ATP[t]}}{0.003}+\frac{\mathrm{pyr[t]}\times\mathrm{ATP[t]}}{0.002\times0.003}}{1+\frac{\mathrm{ADP[t]}}{4.74\times10^{-4}}+\frac{\mathrm{pep[t]}}{2.25\times10^{-4}}+\frac{\mathrm{ADP[t]}\times\mathrm{pep[t]}}{4.74\times10^{-4}\times2.25\times10^{-4}}+\frac{\mathrm{pyr[t]}}{0.002}+\frac{\mathrm{ATP[t]}}{0.003}+\frac{\mathrm{pyr[t]}\times\mathrm{ATP[t]}}{0.002\times0.003}};$$

$$\mathbf{vEN} = 3.43\times10^{-6}\times\left(\frac{458\times\mathrm{NADH[t]}\times\mathrm{pyr[t]}}{2.45\times10^{-6}\times1.37\times10^{-4}}-\frac{115\times\mathrm{NAD[t]}\times\mathrm{lac[t]}}{0.00733\times1.07\times10^{-4}}\right)$$

$$=\frac{\frac{8.44\times10^{-6}\times\mathrm{pyr[t]}}{2.45\times10^{-6}\times1.37\times10^{-4}}+\frac{0.00107\times\mathrm{NAD[t]}}{0.00733\times1.07\times10^{-4}}*\left(1+\frac{\mathrm{pyr[t]}}{1.01\times10^{-4}}\right)+\frac{\mathrm{NADH[t]}}{2.45\times10^{-6}}+\frac{\mathrm{lac[t]}}{0.00733}+\frac{\mathrm{NADH[t]}\times\mathrm{pyr[t]}}{2.45\times10^{-6}\times1.37\times10^{-4}}+\frac{0.00107\times\mathrm{NADH[t]}\times\mathrm{NAD[t]}}{2.45\times10^{-6}\times0.00733\times1.07\times10^{-4}}+}{1+\frac{8.44\times10^{-6}\times\mathrm{pyr[t]}}{2.45\times10^{-6}\times1.37\times10^{-4}}+\frac{0.00107\times\mathrm{NAD[t]}}{0.00733\times1.07\times10^{-4}}*\left(1+\frac{\mathrm{pyr[t]}}{1.01\times10^{-4}}\right)+\frac{\mathrm{NADH[t]}}{2.45\times10^{-6}}+\frac{\mathrm{lac[t]}}{0.00733}+\frac{\mathrm{NADH[t]}\times\mathrm{pyr[t]}}{2.45\times10^{-6}\times1.37\times10^{-4}}+\frac{0.00107\times\mathrm{NADH[t]}\times\mathrm{NAD[t]}}{2.45\times10^{-6}\times0.00733\times1.07\times10^{-4}}+}$$

$$\textbf{vG6PDH} = 6.4\times10^{-5}\times\frac{\frac{\mathrm{NADP[t]}\times\mathrm{g6p[t]}}{3.67\times10^{-6}\times6.67\times10^{-5}}}{1+\left(\frac{\mathrm{NADP[t]}}{3.67\times10^{-6}}\right)\times\left(1+\frac{\mathrm{g6p[t]}}{6.67\times10^{-5}}\right)+\frac{\mathrm{NADPH[t]}}{3.12\times10^{-6}}};\quad \textbf{v6PGLase} = \frac{6.26\times10^{-4}\times\mathrm{gl6p[t]}}{7.99\times10^{-5}+\mathrm{gl6p[t]}};$$

k1 = 2400000; k2 = 410; k3 = 2×10^{9}; k4 = 26000; k5 = 48; k6 = 30; k7 = 630; k8 = 36000; k9 = 800; k10 = 225000; k11 = 300; k12 = 4950000; N1 = k1k3k5k7k9; N2 = k2k4k6k8k10; D1 = k2k9(k4k6 + k5k6 + k5k7); D2 = k1k9(k4k6 + k5k6 + k5k7); D3 = k3k5k7k9; D4 := k2k4k6k8; D5 = k2k10(k4k6 + k5k6 + k5k7); D6 = k1k3(k5k7 + k5k9 + k6k9 + k7k9); D7 = k1k4k6k8; D8 = k3k5k7k10; D9 = k8k10(k2k4 + k2k5 + k2k6 + k4k6); D10 = k1k3k8(k5 + k6); D11 = k3k8k10(k5 + k6);

v6PGODH

$$= \frac{2.1\times10^{-6}\times(\mathrm{N1}\times\mathrm{NADP[t]}\times\mathrm{go6p[t]}-\mathrm{N2}\times\mathrm{ru5p[t]}\times\mathrm{NADPH[t]})}{\mathrm{D1}+\mathrm{D2}\times\mathrm{NADP[t]}+\mathrm{D3}\times\mathrm{go6p[t]}+\mathrm{D4}\times\mathrm{ru5p[t]}+\mathrm{D5}\times\mathrm{NADPH[t]}+\mathrm{D6}\times\mathrm{NADP[t]}\times\mathrm{go6p[t]}+\mathrm{D7}\times\mathrm{NADP[t]}\times\mathrm{ru5p[t]}+\mathrm{D8}\times\mathrm{go6p[t]}\times\mathrm{NADPH[t]}+\mathrm{D9}\times\mathrm{ru5p[t]}\times\mathrm{NADPH[t]}+\\ +\mathrm{D10}\times\mathrm{NADP[t]}\times\mathrm{go6p[t]}\times\mathrm{ru5p[t]}+\mathrm{D11}\times\mathrm{go6p[t]}\times\mathrm{ru5p[t]}\times\mathrm{NADPH[t]}};$$

$$\textbf{vR5PI} = 1.42\times10^{-5}\times\frac{\frac{14.2\times\mathrm{ru5p[t]}}{33.3+14.2}-\frac{33.3\times\mathrm{r5p[t]}}{60900}}{21600};\quad \textbf{vX5PI} = 4.22\times10^{-6}\times\frac{\frac{14.2\times\mathrm{ru5p[t]}}{438+305}-\frac{438\times\mathrm{x5p[t]}}{3910000}}{1490000};$$

$$1+\frac{\mathrm{ru5p[t]}}{33.3+14.2}+\frac{\mathrm{r5p[t]}}{60900}\qquad 1+\frac{\mathrm{ru5p[t]}}{438+305}+\frac{\mathrm{x5p[t]}}{3910000}$$

k1 = 21600; k2 = 45.3; k3 = 16.3; k4 = 30000; k5 = 490000; k6 = 60; k7 := 17; k8 = 79000; M11 = k1k3k5 * k7; M12 = k2k4k6k8; T11 = k1k3(k6 + k7); T12 = k5k7(k2 + k3); T13 = k2k4(k6 + k7); T14 = k6k8(k2 + k3); T15 = k1k5(k3 + k7); T16 = k4k8(k2 + k6); T17 = k5k8(k2 + k3); T18 = k1k4(k6 + k7);

vTA

$$= 6.9\times10^{-7}\times\frac{\mathrm{M11}\times\mathrm{s7p[t]}\times\mathrm{ga3p[t]}-\mathrm{M12}\times\mathrm{e4p[t]}\times\mathrm{f6p[t]}}{\mathrm{T11}\times\mathrm{s7p[t]}+\mathrm{T12}\times\mathrm{ga3p[t]}+\mathrm{T13}\times\mathrm{e4p[t]}+\mathrm{T14}\times\mathrm{f6p[t]}+\mathrm{T15}\times\mathrm{s7p[t]}\times\mathrm{ga3p[t]}+\mathrm{T16}\times\mathrm{e4p[t]}\times\mathrm{f6p[t]}+\mathrm{T17}\times\mathrm{ga3p[t]}\times\mathrm{f6p[t]}+\mathrm{T18}\times\mathrm{s7p[t]}\times\mathrm{e4p[t]}};$$

k1 = 216000; k2 = 38; k3 = 34; k4 = 156000; k5 = 329000; k6 = 175; k7 = 40; k8 = 44800; M21 = k1k3k5k7; M22 = k2k4k6k8; T21 = k1k3(k6 + k7); T22 = k5k7(k2 + k3); T23 = k2k4(k6 + k7); T24 = k6k8(k2 + k3); T25 = k1k5(k3 + k7); T26 = k4k8(k2 + k6); T27 = k5k8(k2 + k3); T28 = k1k4(k6 + k7);

vTK1

$$= 3.3\times10^{-7}\times\frac{\mathrm{M21}\times\mathrm{x5p[t]}\times\mathrm{r5p[t]}-\mathrm{M22}\times\mathrm{ga3p[t]}\times\mathrm{s7p[t]}}{\mathrm{T21}\times\mathrm{x5p[t]}+\mathrm{T22}\times\mathrm{r5p[t]}+\mathrm{T23}\times\mathrm{ga3p[t]}+\mathrm{T24}\times\mathrm{s7p[t]}+\mathrm{T25}\times\mathrm{x5p[t]}\times\mathrm{r5p[t]}+\mathrm{T26}\times\mathrm{ga3p[t]}\times\mathrm{s7p[t]}+\mathrm{T27}\times\mathrm{r5p[t]}\times\mathrm{s7p[t]}+\mathrm{T28}\times\mathrm{x5p[t]}\times\mathrm{ga3p[t]}};$$

k1 = 216000; k2 = 38; k3 = 34; k4 = 156000; k5 = 2240000; k6 = 175; k7 = 40; k8 = 21300; M31 = k1k3k5k7; M32 = k2k4k6k8; T31 = k1k3(k6 + k7); T32 = k5k7(k2 + k3); T33 = k2k4(k6 + k7); T34 = k6k8(k2 + k3); T35 = k1k5(k3 + k7); T36 = k4k8(k2 + k6); T37 = k5k8(k2 + k3); T38 = k1k4(k6 + k7);

vTK2

$$= 3.3\times10^{-7}\times\frac{\mathrm{M31}\times\mathrm{x5p[t]}\times\mathrm{e4p[t]}-\mathrm{M32}\times\mathrm{ga3p[t]}\times\mathrm{f6p[t]}}{\mathrm{T31}\times\mathrm{x5p[t]}+\mathrm{T32}\times\mathrm{e4p[t]}+\mathrm{T33}\times\mathrm{ga3p[t]}+\mathrm{T34}\times\mathrm{f6p[t]}+\mathrm{T35}\times\mathrm{x5p[t]}\times\mathrm{e4p[t]}++\mathrm{T36}\times\mathrm{ga3p[t]}\times\mathrm{f6p[t]}+\mathrm{T37}\times\mathrm{e4p[t]}\times\mathrm{f6p[t]}+\mathrm{T38}\times\mathrm{x5p[t]}\times\mathrm{ga3p[t]}}$$

SPELL: 1. OK